

Gestational exposure of *Ahr* and *Arnt* hypomorphs to dioxin rescues vascular development

Jacqueline A. Walisser, Maureen K. Bunger, Edward Glover, and Christopher A. Bradfield*

McArdle Laboratory for Cancer Research, University of Wisconsin Medical School, Madison, WI 53706

Edited by Ronald M. Evans, The Salk Institute for Biological Studies, La Jolla, CA, and approved October 13, 2004 (received for review June 18, 2004)

The aryl hydrocarbon receptor (AHR) is commonly known for its role in the adaptive metabolism of xenobiotics and in the toxic events that follow exposure to 2,3,7,8-tetrachlorodibenzo-*p*-dioxin (dioxin). Previously, we have demonstrated that the AHR and its heterodimeric partner, the AHR nuclear translocator (ARNT), play a role in the developmental closure of a hepatic vascular shunt known as the ductus venosus (DV). To investigate the mechanism of DV closure, we generated hypomorphic alleles of the *Ahr* and *Arnt* loci. Using these models, we then asked whether this vascular defect could be rescued by receptor activation during late development. By manipulating gestational exposure, the patent DV in AHR or ARNT hypomorphs could be efficiently closed by dioxin exposure as early as embryonic day 12.5 and as late as embryonic day 18.5. These findings define the temporal regulation of receptor activation during normal ontogeny and provide evidence to support the idea that receptor activation and AHR–ARNT heterodimerization are essential for normal vascular development. Taken in the broader context, these data demonstrate that similar AHR signaling steps govern all major aspects of AHR biology.

The biological pathways mediated by the aryl hydrocarbon receptor (AHR) include an adaptive metabolic response to polycyclic aromatic hydrocarbons and a pleiotropic toxic response to more potent agonists such as 2,3,7,8-tetrachlorodibenzo-*p*-dioxin (dioxin) (1–3). Both the adaptive and toxic pathways require ligand activation of the receptor, translocation of the AHR to the nucleus, and dimerization with another basic helix–loop–helix *Per-Arnt-Sim* (PAS) protein known as AHR nuclear translocator (ARNT) (4). Upon exposure to ligands, the AHR dimerizes with ARNT, and the resultant heterodimer binds specific dioxin-responsive enhancer elements to up-regulate a battery of genes encoding xenobiotic metabolizing enzymes (1, 5). The mechanisms by which the AHR mediates toxic responses to potent agonists like dioxin are not well defined. Although we know that many toxic events result from AHR–ARNT dimerization and heterodimeric interaction with dioxin-responsive enhancer elements, it is unclear how specific pathological endpoints such as hepatotoxicity, thymic involution, and epithelial hyperplasia result from the receptor's transcriptional activity (6–9).

Recently, it has been shown that the AHR also mediates a third pathway best defined as “developmental.” The most robust phenotype arising from the generation of null alleles at the *Ahr* locus is a reduced liver size (10–13). Our laboratory has investigated the cause of this atrophy and identified a congenital vascular defect, failure of ductus venosus (DV) closure. The DV is a fetal hepatic shunt that normally closes in the first days after birth. In *Ahr*-null mice, this structure remains patent (open), resulting in significant porto-caval shunting and aberrant hepatic blood flow throughout adult life (10). Recently, we have provided evidence that the ARNT protein and AHR's ability to localize to the nucleus are also required for normal DV closure (6, 7). Taken in sum, these findings provide evidence that the developmental pathway bears some mechanistic resemblance to the adaptive and toxic pathways.

Given the clear role of ligand binding in the adaptive and toxic pathways, we set out to find evidence for the importance of

receptor activation in normal vascular development. That is, we began a search for an endogenous ligand or endogenous receptor activator using developmental closure of the DV as the biologically relevant endpoint. To this end, we generated hypomorphic *Ahr* and *Arnt* alleles that allowed us to examine the outcome of limiting AHR or ARNT protein on the developmental aspects of AHR signal transduction. Using these hypomorphic models, we provide evidence that receptor activation and developmentally induced heterodimerization with ARNT are normal features of the receptor pathway driving vascular resolution. Taken in sum, these data provide a powerful example of how differential timing or extent of activation of a single receptor can lead to three distinct biological outcomes, i.e., up-regulation of xenobiotic metabolism, dioxin toxicity, and normal vascular development.

Materials and Methods

Generation of Hypomorphic *Ahr* Mice. The strategy used to generate the hypomorphic *Ahr* allele is similar to that described previously for generation of a hypomorphic *Arnt* allele (*Arnt^{flneo}*) (6). A P1-bacteriophage clone containing a 15-kb region of homology to the murine *Ahr* locus was obtained from a 129SvJ genomic library (Genome Systems, St. Louis) (14). The 129SvJ strain carries the *Ahr^d* allele of the *Ahr* locus (15). For construction of the hypomorphic *Ahr* allele, we flanked exon 2 with *loxP* sites (“floxed”). Exon 2 was targeted because it encodes the basic helix–loop–helix domain essential for DNA binding (16, 17). To aid in screening of homologous recombinants, a *Bam*HI site was engineered adjacent to the *loxP* site downstream of exon 2. This targeting vector also contains the positive selection marker, the neomycin resistance gene (*Neo*), which is flanked by *loxP* sites, and the negative selection marker thymidine kinase. The final targeting construct was designated PL1737. Homologous recombination protocols using GS1 embryonic stem cells (Genome Systems) have been described previously (7). Clones were screened for homologous recombination by Southern blot of *Bam*HI-digested genomic DNA using an 800-bp probe (PL311) located 3' to the end of the targeting construct. Targeted clones were injected into 3.5-day postcoital C57BL/6J blastocysts, and resulting chimeras were backcrossed to C57BL/6J mice to determine germ-line transmission of the targeted allele. Animals transmitting the mutation, designated *Ahr^{flneo}*, which included the floxed *Neo* marker gene, were backcrossed to the C57BL/6J strain congenic for the DBA2-derived *Ahr^d* allele (see *Animals*) for two to five generations before experimental analysis. Genotyping was routinely performed by PCR on DNA isolated from tail biopsies by using the forward primer OL4064 (5'-CAGTGGGAATAAGGCAAGAGTGA) and the reverse primer OL4088 (5'-GGTACAAGTGCACATGCCTGC).

This paper was submitted directly (Track II) to the PNAS office.

Abbreviations: AHR, aryl hydrocarbon receptor; dioxin, 2,3,7,8-tetrachlorodibenzo-*p*-dioxin; DV, ductus venosus; EROD, ethoxyresorufin *O*-deethylase; ARNT, AHR nuclear translocator; *En*, embryonic day *n*.

*To whom correspondence should be addressed at: McArdle Laboratory for Cancer Research, 1400 University Avenue, Madison, WI 53706. E-mail: bradfield@oncology.wisc.edu.

© 2004 by The National Academy of Sciences of the USA

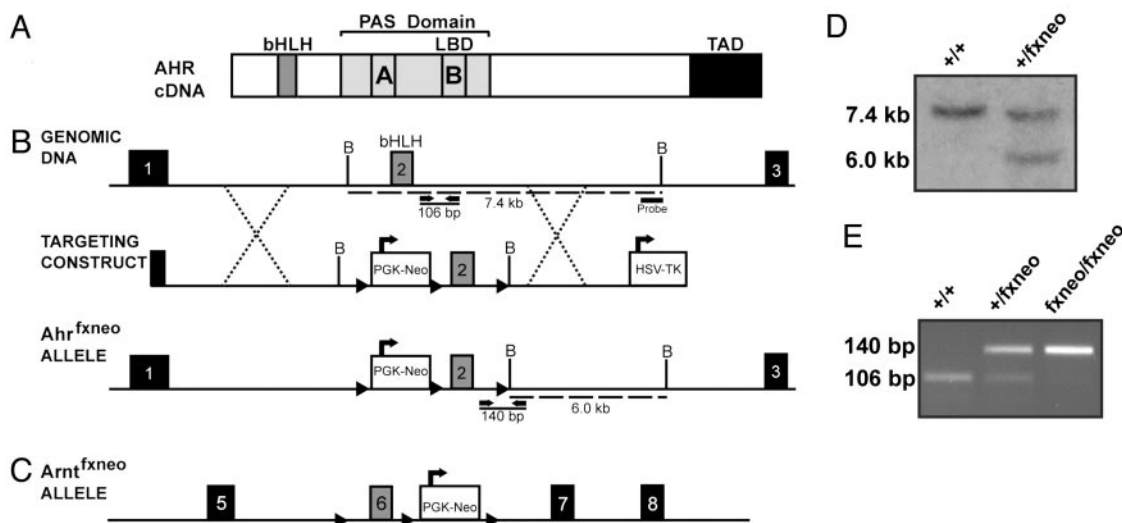


Fig. 1. Generation of *Ahr^{fxneo}* mice. (A) Schematic diagram of the *Ahr* cDNA identifying important functional domains including the basic helix–loop–helix (bHLH) domain, the *Per-Arnt-Sim* (PAS) domain with A and B repeats, and the transactivation domain (TAD). (B) Schematic diagram illustrating the region surrounding the bHLH domain of the murine *Ahr* locus, the targeting construct, and the resulting hypomorphic *Ahr^{fxneo}* allele. Exon numbers reflect known coding exons. To generate the hypomorphic *Ahr* allele, the *Neo* gene was inserted upstream of exon 2, and both *Neo* and exon 2 were flanked with *loxp* sites. Dotted lines indicate regions of homology used for homologous recombination. Dashed lines indicate fragment sizes detected by the probe after digestion of genomic DNA with *Bam*HI. Solid lines represent the fragment sizes generated by PCR genotyping of the wild-type and hypomorphic alleles using OL4064 as the forward primer and OL4088 as the reverse primer. (C) Schematic diagram of the *Arnt^{fxneo}* hypomorphic allele. (D) Southern blot of mouse tail biopsies showing bands of 7.4 kb and 6.0 kb, indicating the presence of the wild-type and mutant alleles, respectively. (E) PCR genotyping of tail biopsies showing bands of 106 bp and 140 bp, indicating the presence of the wild-type and mutant alleles, respectively.

These primers amplified a 106-bp band from the wild-type allele and a 140-bp band from the targeted allele because of the insertion of the *loxp* site. The PCR was carried out for 29 cycles (95°C for 30 s, 60°C for 30 s, and 72°C for 30 s) in a reaction mixture containing 2.5 units of *Taq* polymerase (Promega), 50 mM KCl, 10 mM Tris-HCl (pH 9.0 at 25°C), 1.5 mM MgCl₂, 1% Triton X-100, 200 μM dNTPs, and 0.2 μM each primer.

Animals. Mice were housed in a selective pathogen-free facility on corn cob bedding with food and water ad libitum according to the rules and guidelines set by the University of Wisconsin. Because of the fact that the 129SvJ embryonic stem cells carry the lower-affinity *Ahr^d* allele, we used a C57BL/6J strain congenic for the DBA2-derived *Ahr^d* allele to perform all backcrosses of the *Ahr^{fxneo}* allele and as experimental controls (15). For clearer presentation, the wild-type *Ahr^d* allele is referred to as *Ahr⁺* (“wild-type”) throughout this paper.

Characterization of the *Ahr^{fxneo}* Allele. Expression of the AHR protein was evaluated in mice homozygous for the wild-type (*Ahr^{+/+}*) or the *Ahr^{fxneo}* allele (*Ahr^{fxneo/fxneo}*) by Western blot analysis of cytosolic fractions prepared from various tissues including the liver, kidney, spleen, heart, and lung (7, 18). To estimate the amount of AHR protein expressed in various tissues, standards were prepared from dilutions of liver extracts from wild-type animals. For P450 induction studies, 12-week-old mice were dosed once by i.p. injection with 100 μg/kg dioxin in DMSO or with DMSO alone. Ethoxyresorufin *O*-deethylase (EROD) assays were performed on microsomal liver fractions to assess P450 induction (7, 18). In situations where multiple comparisons could be made, an ANOVA was performed and Tukey’s test was used to determine differences with a *P* ≤ 0.05.

Rescue of the DV. Matings between *Ahr^{fxneo/+}* females and *Ahr^{fxneo/fxneo}* males were performed for a 14- to 16-h period overnight, and the females were removed the following morning. The day the female was removed was defined as embryonic

day (E) 0.5. Embryos generated from these crosses were either *Ahr^{fxneo/+}* heterozygotes or *Ahr^{fxneo/fxneo}* homozygotes. For experiments designed to test for closure of the DV through dioxin exposure, we dosed pregnant *Ahr^{fxneo/+}* females at E12.5, E14.5, E16.5, or E18.5 with 25 μg/kg dioxin in DMSO or with DMSO alone by i.p. injection. After *in utero* exposure to dioxin, pups were allowed to reach ≈4–6 weeks of age, and their DV status was assessed by liver perfusion (see *Assessment of DV Status*). Rescue experiments using the ARNT hypomorphs were performed in a similar manner, with treatment of pregnant females occurring on E16.5. Rescue experiments were also performed on *Ahr*-null mice. For these experiments, pregnant *Ahr*-null females that had been mated to *Ahr*-null males were injected with dioxin or vehicle on E18.5.

Assessment of DV Status. The status of the DV was assessed by perfusion of the liver with Trypan blue (10). Livers were cannulated by means of the portal vein, and the inferior vena cava was incised to permit outflow. Once the livers were flushed with PBS, ≈0.5 ml of Trypan blue was injected. Upon injection of the dye, failure of the liver to turn blue, combined with confirmation of Trypan blue outflow from the inferior vena cava, indicated a patent (open) DV. In some cases, this analysis was confirmed by time-lapsed angiography. To accomplish this, the Omnipaque 300 contrast agent (Nycomed, Princeton) was injected into the portal vein, and continuous x-ray images were obtained over 5 s (10). This procedure allowed visualization of the liver vascular architecture and confirmation of DV status (open or closed).

Results

Generation of *Ahr^{fxneo}* Mice. In an effort to engineer an allele that both was hypomorphic and held the potential for later conditional deletion, we designed the *Ahr* mutation to include a *Neo* cassette flanked by *loxp* sites. This “floxed-*Neo*” insertion was placed adjacent to exon 2, which encodes the basic helix–loop–helix of *Ahr* (Fig. 1B). A third *loxp* site was inserted downstream

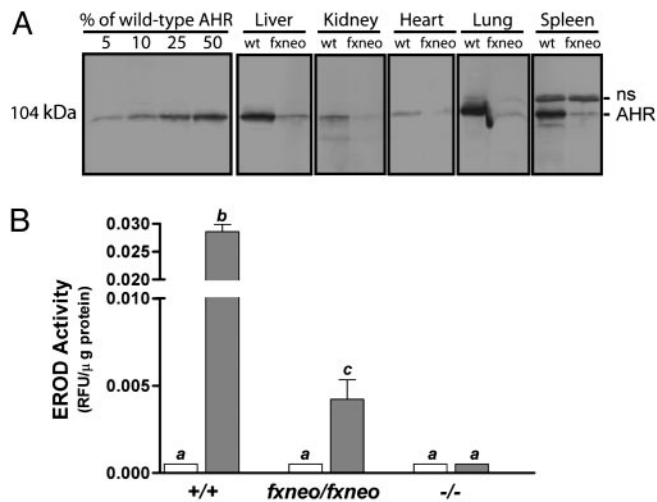


Fig. 2. The *Ahr^{fxneo}* allele is hypomorphic. (A) Western blot analyses showing AHR protein levels in cytosolic extracts from wild-type (wt) and *Ahr^{fxneo/fxneo}* (*fxneo*) mice prepared from liver, kidney, spleen, heart, and lung. Molecular mass reflects the *Ahr^d* allele. Standards prepared from dilutions of liver extracts from wild-type animals were included to estimate the amount of protein expressed in various tissues. ns, nonspecific protein band identified by reaction with preimmune sera (data not shown). (B) The *Ahr^{fxneo}* allele is hypomorphic in function. Liver microsomes from 12-week-old wild-type (+/+), *Ahr^{fxneo/fxneo}*, and *Ahr^{-/-}* mice were prepared 7 days after treatment with 100 μg/kg dioxin in DMSO or with DMSO alone. Microsomal isolations were incubated with ethoxyresorufin in the presence of NADPH. EROD activity was measured from vehicle- and dioxin-treated animals at an excitation of 510 nm and an emission of 590 nm. Fluorescent values were normalized to total protein levels. The wild-type and *Ahr*-null groups each contain five animals, whereas the *Ahr^{fxneo/fxneo}* groups each contain four animals. White bars, vehicle-treated animals; gray bars, dioxin-treated animals. Error bars indicate standard error. Those groups not sharing a superscript letter differ significantly at $P \leq 0.05$.

of exon 2 for later creation of the conditional null. A map of the targeted *Ahr* allele, *Ahr^{fxneo}*, is shown in Fig. 1B. Also shown is a map of the *Ahr* structural gene, as well as the construct used for embryonic stem cell targeting. For comparison, a map of the hypomorphic ARNT allele (*Arnt^{fxneo}*), generated previously (6), is also shown (Fig. 1C).

After homologous recombination in embryonic stem cells, surviving clones were screened by Southern blot analysis (Fig. 1D). Correctly targeted clones were used to generate chimeras, and these mice provided germ-line transmission of the *Ahr^{fxneo}* allele. A PCR-based protocol was developed to genotype pups based on detection of the *loxP* sequence downstream of exon 2 (Fig. 1E). The outcome of our *Ahr^{fxneo}* breeding program demonstrated compliance with the Mendelian ratios predicted for a nonlethal mutation. That is, wild-type (*Ahr^{+/+}*), heterozygous (*Ahr^{fxneo/+}*), and homozygous (*Ahr^{fxneo/fxneo}*) pups were born at the expected 1:2:1 ratio. Actual numbers from heterozygous crosses were 26% (20/77) wild type, 51% (39/77) *Ahr^{fxneo/+}*, and 23% (23/77) *Ahr^{fxneo/fxneo}*. Males and females were produced in equal proportions and were outwardly normal and fertile as adults.

The *Ahr^{fxneo}* Allele Is Hypomorphic. We examined the influence of this mutation on AHR protein expression by Western blot analysis of protein extracts derived from various tissues prepared from wild-type mice and mice homozygous for the *Ahr^{fxneo}* allele (i.e., *Ahr^{fxneo/fxneo}*). This analysis revealed that expression of the 104-kDa AHR protein (derived from the *Ahr^d* allele) was significantly diminished in all tissue samples analyzed, including liver, kidney, spleen, heart, and lung (Fig. 2A). Based on

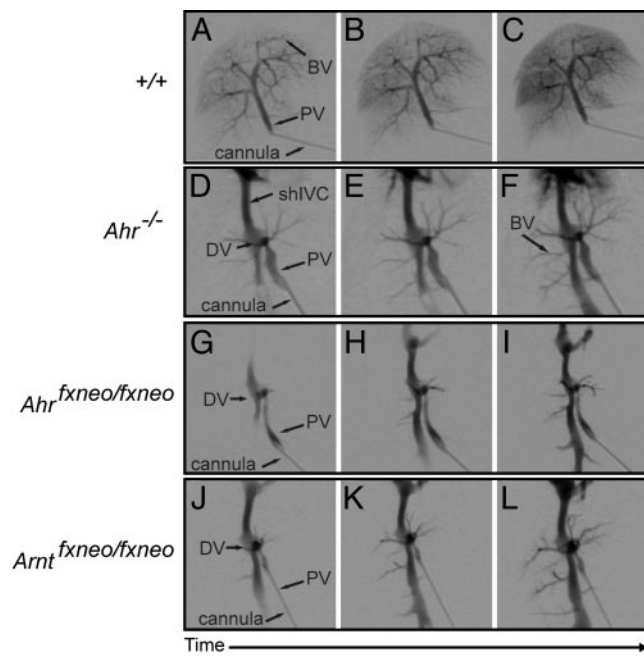


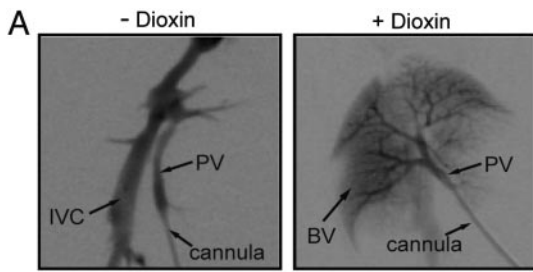
Fig. 3. Porto-caval shunting and patent DV in *Ahr^{fxneo}* hypomorphs mimic the *Ahr*-null liver vascular phenotype. Time-lapsed radiographs of the liver vascular system after injection of contrast agent into the portal vein of wild-type (A–C), *Ahr^{-/-}* (D–F), *Ahr^{fxneo/fxneo}* (G–I), and *Arnt^{fxneo/fxneo}* (J–L) mice. Arrows indicate key anatomical features of the liver: PV, portal vein; shIVC, suprahepatic inferior vena cava; BV, branching vessels.

comparison with dilutions of tissue extracts from wild-type animals, we estimate that AHR protein expression in all tissues examined from *Ahr^{fxneo/fxneo}* mice was reduced to <10% of wild-type levels. This experiment establishes that the *Ahr^{fxneo}* allele is globally hypomorphic for AHR protein expression. Thus, we refer to the *Ahr^{fxneo}* allele as the AHR hypomorph.

The decrease in protein expression from the *Ahr^{fxneo}* allele led us to ask whether signal transduction through the AHR pathway would be compromised. Therefore, we compared the response of *Ahr^{+/+}*, *Ahr^{fxneo/fxneo}*, and *Ahr^{-/-}* mice to a single dose of 100 μg/kg dioxin. Seven days after dioxin treatment, liver microsomes were prepared and the adaptive metabolic response of P450 induction was measured. In the liver, the classic AHR-induced adaptive response to dioxin exposure includes the up-regulation of CYP1A1 and CYP1A2 enzymes, the composite of which is measured as EROD activity. Microsomes from all groups showed negligible EROD activity in the absence of the AHR ligand, dioxin (Fig. 2B). As expected, microsomes from *Ahr^{-/-}* mice showed no induction above background levels in response to dioxin. In contrast, microsomes from *Ahr^{fxneo/fxneo}* mice showed measurable EROD activity in response to dioxin; however, this activity was ≈7-fold lower than that observed for wild-type mice ($P < 0.001$).

Vascular Phenotype of *Ahr^{fxneo}* Mice Mimics That of *Ahr*-Null Mice.

Because of our previous demonstration of the importance of the AHR in the closure of the DV, we asked whether this shunt was also present in hypomorphic *Ahr^{fxneo}* animals (10). Time-lapse radiographs of the liver vascular system illustrate the normal liver vascular pattern of adult wild-type mice where injection of contrast agent into the portal vein rapidly fills both primary and secondary branches of the liver (Fig. 3A–C). By comparison, contrast agent injected into the portal vein of the *Ahr*-null mouse flows directly between the portal vein and the inferior vena cava, illustrating a direct shunt consistent with



B

Pup Genotype	Time of Treatment	DMSO		Dioxin	
		DV Closure	%	DV Closure	%
<i>Ahr^{fxneo/fxneo}</i>	E12.5	2/15	13	11/11	100
	E14.5	0/12	0	12/12	100
	E16.5	0/9	0	21/21	100
	E18.5	0/11	0	18/18	100
<i>Arnt^{fxneo/fxneo}</i>	E16.5	1/12	8	17/17	100
<i>Ahr^{-/-}</i>	E18.5	0/12	0	0/11	0

Fig. 4. Embryonic exposure to dioxin leads to DV closure in *Ahr^{fxneo}* and *Arnt^{fxneo}* hypomorphs. Timed matings of heterozygous (*Ahr^{fxneo/+}*) AHR hypomorph females and homozygous (*Ahr^{fxneo/fxneo}*) AHR hypomorph males were performed. At various stages of gestation, pregnant females were given an i.p. injection of 25 μ g/kg dioxin or vehicle (DMSO) alone. The DV status of the resulting progeny was assessed by radiography or Trypan blue liver perfusion when the pups were 4–6 weeks old. Similar studies were performed with the ARNT hypomorphs and *Ahr*-null mice, and injections of pregnant females were performed at E16.5 and E18.5, respectively. Approximately half of the *Ahr*-null mice in the vehicle group received DMSO at E18.5, while the other half received no treatment during development. (A) Liver vascular architecture of an untreated *Ahr^{fxneo/fxneo}* hypomorph (Left) and an *Ahr^{fxneo/fxneo}* hypomorph after *in utero* exposure to dioxin at E14.5 (Right). (B) Frequency of DV closure in adult AHR *Ahr^{fxneo}* hypomorphs, *Arnt^{fxneo}* hypomorphs, and *Ahr*-null mice after *in utero* exposure to either dioxin or vehicle (DMSO) at various stages of gestation.

the existence of a patent DV (Fig. 3 D–F) (10). Similar to the *Ahr*-null mice, injection of contrast agent into the portal vein of the *Ahr^{fxneo/fxneo}* mice revealed a vascular pattern consistent with a patent DV (Fig. 3 G–I). This phenotype is independent of sex of the animal (data not shown). These data demonstrate that both the AHR hypomorphs and the *Ahr*-null mice display identical vascular deficits, i.e., porto-caval shunting, consistent with a patent DV.

The sum of our Trypan blue perfusion and autoradiography experiments demonstrates that three distinct mutations in the AHR signaling pathway (*Ahr*-null, *Ahr^{fxneo}*, and *Arnt^{fxneo}*) generate a qualitatively similar pattern of porto-caval shunting. That is, a direct radiographic comparison of vascular flow in the *Ahr*-null, *Ahr^{fxneo}*, and *Arnt^{fxneo}* mice yields essentially identical images of the putative DV (Fig. 3 D–L) (6). Although the shunt is qualitatively similar in these three mutants, its penetrance is quantitatively different. In this regard, larger-scale studies using Trypan blue liver perfusion as an endpoint revealed a frequency of DV closure of $\approx 12\%$ (3/25) in the *Ahr^{fxneo/fxneo}* mice (data not shown). By comparison, the frequency of DV closure in *Ahr*-null mice is 0% (0/12) (Fig. 4B) (10). In these experiments, we observed a frequency of DV closure of $\approx 8\%$ (1/12) in hypomorph *Arnt^{fxneo}* mice (Fig. 4B).

Embryonic Dioxin Exposure Leads to DV Closure in AHR Hypomorphs.

Given that both the adaptive and toxic pathways of AHR signal transduction begin with ligand activation of the receptor, we postulated that the same would be true for closure of the DV (i.e., the developmental pathway). To test this idea, we exposed

Ahr^{fxneo/+} and *Ahr^{fxneo/fxneo}* pups *in utero* to dioxin or vehicle (DMSO) at various stages of gestation and evaluated their DV status at 4–6 weeks of age. The dose of dioxin administered to the female did not cause maternal toxicity, nor was it high enough to induce the teratogenic endpoints of cleft palate and hydronephrosis in the hypomorph pups (19). To assess DV status of mice, we performed time-lapse autoradiography and found that AHR hypomorphs exposed to dioxin as embryos displayed a liver vasculature consistent with normal developmental closure of the DV (Fig. 4A). Complete rescue of the DV phenotype was achieved in AHR hypomorphs independent of the time of dioxin exposure (Fig. 4B). For example, 100% DV closure was observed when animals were exposed to dioxin at E12.5, E14.5, E16.5, or E18.5. This finding compares with a $<13\%$ rate of DV closure in *Ahr^{fxneo/fxneo}* animals that were treated *in utero* with DMSO (Fig. 4B). Liver perfusions on *Ahr^{fxneo/+}* pups demonstrated that a single wild-type *Ahr* allele was sufficient to confer a wild-type liver vascular phenotype that was unaffected by dioxin exposure (data not shown). Finally, to demonstrate that the rescue experiments depended on AHR, we treated *Ahr^{-/-}* embryos *in utero* with dioxin or vehicle at E18.5 and observed complete failure of the DV to close (0/11) (Fig. 4B).

Embryonic Dioxin Exposure Leads to DV Closure in ARNT Hypomorphs.

Given the observation that the vascular phenotype of AHR hypomorphs can be rescued by embryonic exposure to dioxin, we then examined the possibility that the vascular phenotype of our previously described ARNT hypomorphs (*Arnt^{fxneo}*) could be similarly rescued. To address this question, ARNT hypomorphs were exposed to dioxin or DMSO *in utero*, and their DV status was assessed as adults. The frequency of DV closure in *Arnt^{fxneo/fxneo}* embryos treated *in utero* with the vehicle, DMSO, was $\approx 8\%$. As observed with the AHR hypomorphs, dioxin exposure at E16.5 also results in a complete closure of the DV in ARNT hypomorphs (Fig. 4B).

Discussion

The AHR signal transduction pathway can be viewed as a trilogy. This receptor mediates three physiological processes: (i) the adaptive pathway ensuring up-regulation of xenobiotic metabolizing enzymes in response to polycyclic aromatic hydrocarbon exposure, (ii) the toxic pathway mediating the deleterious effects of high-affinity agonists, like dioxin, and (iii) the developmental pathway directing normal vascular architecture in response to an unknown developmental cue (4, 6). Given that both the adaptive and toxic response pathways of the AHR have been shown to require receptor activation by a ligand, translocation of the AHR to the nucleus, heterodimerization with ARNT, and binding to specific DNA enhancers, we hypothesized that the developmental pathway would proceed in a similar manner. To test this idea, we set out to demonstrate that receptor activation and ARNT heterodimerization were necessary aspects of the developmental pathway.

In an effort to investigate the developmental aspects of AHR signaling, we generated a hypomorphic allele of the *Ahr* locus. We postulated that a hypomorphic allele of *Ahr* would provide us with a level of control over receptor-dependent developmental events. Specifically, we hypothesized that this allele would result in attenuated developmental phenotypes. We predicted that this model would provide a powerful tool to investigate various aspects of AHR biology because it would be more sensitive to chemical and genetic modifiers. In the first stage of this work, we demonstrated that the *Ahr^{fxneo}* hypomorphic model has an attenuated response to dioxin exposure and displays incomplete penetrance with respect to the patent DV phenotype (Fig. 2 and data not shown). We then used patency of the DV as a vascular endpoint to determine whether the developmental

defects observed in the AHR hypomorphs might be rescued by receptor activation.

AHR-Dependent Developmental Signaling. The use of this hypomorphic approach allowed us to demonstrate that, when the AHR is limiting, perinatal dioxin exposure rescues the hallmark developmental aberration seen in *Ahr*-null mice, a patent DV. These experiments led to three important observations related to AHR signaling in normal development. First, these experiments demonstrate that there is a threshold level of AHR protein that is necessary to achieve DV closure. This argument is supported by the observation that AHR hypomorphs display a low frequency of DV closure (<13%, Fig. 4B), in contrast to the complete failure of the DV to close in the corresponding null allele (Fig. 4B) (10). Second, the timing of dioxin exposure helps define a temporal window where the activity of the AHR is essential for normal development. In this regard, dioxin exposure between E12.5 and E18.5 resulted in complete closure of the DV in AHR hypomorphs. The ability to achieve closure of the DV as late as E18.5 indicates a critical window of AHR activation at this late stage of development. This late-stage role in vascular development is consistent with previous work demonstrating that closure of the DV is a postpartum event (20). Given that the half-life of dioxin in mice is estimated to be 10–15 days, the ability to rescue the DV phenotype with dioxin administration as early as E12.5 may be a function of its persistence and its ability to activate AHR signaling at subsequent developmental times (21, 22). Third, through *in utero* exposure of AHR hypomorphs to dioxin, we have provided evidence to support the idea that receptor activation is a central feature of normal vascular development. That is, the *Ahr*^{fxneo} embryos, expressing 10% of wild-type AHR, are able to generate a sufficient developmental signal only in the presence of a potent activator.

ARNT-Dependent Developmental Signaling. Using the ARNT hypomorph model, we were able to provide evidence that normal DV closure during development requires not only activation of the AHR but also the recruitment of ARNT. Our previous observation that the DV was present in the ARNT hypomorphs demonstrated that the ARNT hypomorph has a DV phenotype that is essentially identical to that of the *Ahr*-null mice (6). These data provide strong evidence that ARNT is involved in AHR's developmental pathway. Such experiments support the hypothesis that AHR–ARNT heterodimerization is an essential step for developmental closure of the DV. If this model is correct, then it follows that DV closure in ARNT hypomorph animals would also be achieved by perinatal exposure to dioxin. In support of this hypothesis, we demonstrated that complete closure of the DV occurred in ARNT hypomorphs exposed to dioxin at E16.5. Taken in sum, these findings provide evidence that AHR–ARNT heterodimerization is an essential feature of liver vascular resolution.

Endogenous AHR Activators in Development. The demonstration that perinatal dioxin exposure in AHR and ARNT hypomorphs rescues the patent DV phenotype is consistent with the idea that an unknown endogenous activator of this pathway participates in normal developmental signaling. The dioxin-induced rescue of the DV phenotype in both AHR and ARNT hypomorphs implies

that the endogenous activator may be less potent or less efficacious than this xenobiotic agonist. That is, although endogenous activation may still be occurring in AHR and ARNT hypomorphs, this activation is apparently insufficient to close the DV under limiting conditions. The observation that dioxin corrects a physiological deficit is in stark contrast to the more commonly studied deleterious properties of this environmental pollutant. Use of dioxin as a pharmacological rescue suggests that chemicals of this class may have future therapeutic potential, in particular for diagnosed developmental vascular deficits such as a patent DV (23).

A Model for DV Closure. There are a number of models that may explain the developmental role of the AHR signaling pathway. The first model proposes that developmental signaling is essentially identical to the adaptive pathway. That is, enzymes commonly thought of for their role in xenobiotic metabolism may also play a direct role in vascular development. In such a model, developmental AHR signaling leads to induction of the “adaptive” gene battery and the up-regulation of metabolic capacity. One possibility is that a vasoactive compound is either produced or destroyed through P450–1 metabolism, allowing normal vascular remodeling. A second model is that developmental receptor activation leads to the up-regulation of a unique set of dioxin-responsive enhancer element-driven genes, resulting in DV closure. Under this model, we would predict that the relevant AHR–ARNT target genes are under developmental and tissue-specific control that is different from the commonly studied adaptive gene battery.

Conclusions

In conclusion, we have described the generation of a hypomorphic *Ahr*^{fxneo} allele that is globally limiting in receptor expression and displays attenuated signaling. The design of this allele and the incorporation of excisable *loxP* sites will also permit a detailed examination of the tissue specificity of AHR biology in future experiments. Using hypomorphic models of AHR and ARNT, we have provided evidence that ligand activation of AHR and receptor dimerization with ARNT are central features directing developmental resolution of the DV. These findings illustrate the idea that all aspects of AHR biology are governed by a similar series of mechanistic steps. These steps include receptor activation, nuclear translocation of the receptor, heterodimerization with ARNT, and transcriptional up-regulation of gene batteries. Although the mechanism of adaptive, toxic, and developmental signaling appears the same, the outcome of each of these pathways is distinct. How the AHR is able to produce three distinct biological events from a similar signal transduction mechanism is unclear at present. We propose that the distinct outcomes of AHR signaling are each dependent on the interplay of factors that include agonist potency, developmental timing of receptor activation, and the cell or tissue type responding.

We thank Norman Drinkwater and Henry Pitot for valuable scientific input and Laura Green for technical assistance. This work was supported by National Institutes of Health Grants ES006883, CA014520, and CA022484. J.A.W. is the recipient of a postdoctoral fellowship from the Natural Sciences and Engineering Research Council of Canada. M.K.B. was a Mary Engsborg Fellow.

- Schmidt, J. V. & Bradfield, C. A. (1996) *Annu. Rev. Cell Dev. Biol.* **12**, 55–89.
- Whitlock, J. P., Jr., Chichester, C. H., Bedgood, R. M., Okino, S. T., Ko, H. P., Ma, Q., Dong, L., Li, H. & Clarke-Katzenberg, R. (1997) *Drug Metab. Rev.* **29**, 1107–1127.
- Poland, A. & Knutson, J. C. (1982) *Annu. Rev. Pharmacol. Toxicol.* **22**, 517–554.
- Gu, Y.-Z., Hogenesch, J. & Bradfield, C. (2000) *Annu. Rev. Pharmacol. Toxicol.* **40**, 519–561.

- Hankinson, O. (1995) *Annu. Rev. Pharmacol. Toxicol.* **35**, 307–340.
- Walisser, J. A., Bunger, M. K., Glover, E., Harstad, E. B. & Bradfield, C. A. (2004) *J. Biol. Chem.* **279**, 16326–16331.
- Bunger, M. K., Moran, S. M., Glover, E., Thomae, T. L., Lahvis, G. P., Lin, B. C. & Bradfield, C. A. (2003) *J. Biol. Chem.* **278**, 17767–17774.
- Tomita, S., Jiang, H., Ueno, T., Takagi, S., Tohi, K., Maekawa, S., Miyatake, A., Furukawa, A., Gonzalez, F. J., Takeda, J., et al. (2003) *J. Immunol.* **171**, 4113–4120.

9. Uno, S., Dalton, T. P., Sinclair, P. R., Gorman, N., Wang, B., Smith, A. G., Miller, M. L., Shertzer, H. G. & Nebert, D. W. (2004) *Toxicol. Appl. Pharmacol.* **196**, 410–421.
10. Lahvis, G. P., Lindell, S. L., Thomas, R. S., McCuskey, R. S., Murphy, C., Glover, E., Bentz, M., Southard, J. & Bradfield, C. A. (2000) *Proc. Natl. Acad. Sci. USA* **97**, 10442–10447.
11. Fernandez-Salguero, P. M., Hilbert, D. M., Rudikoff, S., Ward, J. M. & Gonzalez, F. J. (1996) *Toxicol. Appl. Pharmacol.* **140**, 173–179.
12. Fernandez-Salguero, P. M., Ward, J. M., Sundberg, J. P. & Gonzalez, F. J. (1997) *Vet. Pathol.* **34**, 605–614.
13. Mimura, J., Yamashita, K., Nakamura, K., Morita, M., Takagi, T. N., Nakao, K., Emak, M., Sogawa, K., Yasuda, M., Katsuki, M. & Fujii-Kuriyama, Y. (1997) *Genes Cells* **2**, 645–654.
14. Schmidt, J. V., Su, G. H., Reddy, J. K., Simon, M. C. & Bradfield, C. A. (1996) *Proc. Natl. Acad. Sci. USA* **93**, 6731–6736.
15. Poland, A. & Glover, E. (1980) *Mol. Pharmacol.* **17**, 86–94.
16. Fukunaga, B. N. & Hankinson, O. (1996) *J. Biol. Chem.* **271**, 3743–3749.
17. Fukunaga, B. N., Probst, M. R., Reisz-Porszasz, S. & Hankinson, O. (1995) *J. Biol. Chem.* **270**, 29270–29278.
18. Schmidt, J. V., Carver, L. A. & Bradfield, C. A. (1993) *J. Biol. Chem.* **268**, 22203–22209.
19. Thomae, T. L., Glover, E. & Bradfield, C. A. (2004) *J. Biol. Chem.* **279**, 30189–30194.
20. Edelstone, D. I. (1980) *J. Dev. Physiol.* **2**, 219–238.
21. Gasiewicz, T. A., Geiger, L. E., Rucci, G. & Neal, R. A. (1983) *Drug Metab. Dispos.* **11**, 397–403.
22. DeVito, M. J. & Birnbaum, L. S. (1995) *Fund. Appl. Toxicol.* **24**, 145–1488.
23. Yoshimoto, Y., Shimizu, R., Saeki, T., Harada, T., Sugio, Y., Nomura, S. & Tanaka, H. (2004) *J. Pediatr. Surg.* **39**, E1–E5.